Silicon-on-insulator electro-optically tunable waveguide-coupled microdisk resonators with selectively integrated p-i-n diodes

Linjie Zhou and Andrew W. Poon

Department of Electrical and Electronic Engineering, The Hong Kong University of Science and Technology,

Clear Water Bay, Hong Kong SAR, China

Tel: (852)-2358-7905; Fax:(852)-2358-1485; Email: eeawpoon@ust.hk

Abstract: We report silicon-on-insulator electro-optically tunable microdisk resonators with selectively integrated p-i-n diodes. Using free-carrier plasma dispersion effect, we show that the whispering-gallery modes can be blueshifted by 0.4 nm upon 1-V forward bias.

@2005 Optical Society of America

OCIS codes: (230.5750) Resonators; (230.2090) Electro-optical devices

Active silicon photonic devices such as electro-optical tunable filters, switches and modulators have been attracting considerable interest [1]. In order to obtain high-speed electro-optical effects in silicon-based devices, the conventional method is to induce free-carrier plasma dispersion effect along mm-cm long waveguide phase-shifter by means of an integrated forward biased p-i-n diode. Most recently, Xu et al [2] demonstrated that silicon electro-optic modulator can be made micrometer-scale by using a microring resonator integrated with a lateral p-i-n diode.

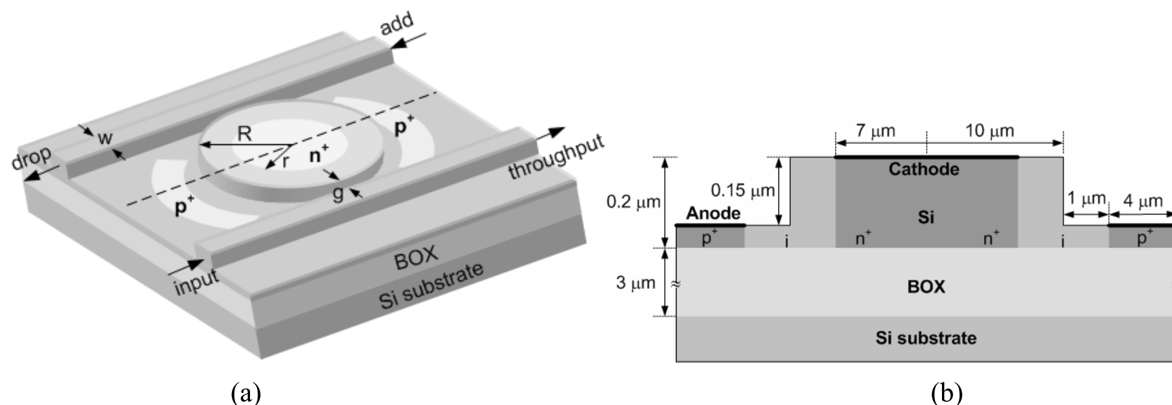

(a) (b)

Fig.1. (a) Schematic of the SOI electro-optically tunable microdisk channel add-drop filter. The lateral p-i-n diode is selectively integrated in order to preferentially inject carriers into the microdisk rim region. (b) Schematic cross-section of the lateral p-i-n diode integrated microdisk along the dashed line in (a).

In this summary, we report initial experimental demonstration of silicon-on-insulator (SOI) electro-optically tunable microdisk resonators with selectively integrated lateral p-i-n diodes. In contrast to microring resonators, microdisk resonators have the potential key merits of high-Q whispering-gallery modes (WGMs), and less sidewall-roughness induced scattering loss due to the absence of an inner sidewall. However, microdisk resonators are multimode, and thus more detailed device design considerations are needed in order to control or tailor the

multimode responses.

Figure 1 (a) shows the schematic of p-i-n diodes integrated active microdisk resonator laterally input and output-coupled with waveguides. We selectively embed a heavily doped n-type region in the microdisk central region and a heavily doped p-type region in the slab region outside the microdisk. This constitutes lateral p-i-n diodes with the microdisk rim as the intrinsic regions. As the WGMs are nearly confined and localized along the microdisk rim intrinsic regions, free-carrier absorption and scattering due to the n^+ and p^+ regions should be minimal and can be engineered (by varying the doped-region radius and the separation from the p^+ arc region). Moreover, as higher order WGM fields extend deeper into the microdisk, it is possible to selectively suppress higher order modes by means of the excess loss in the n^+-doped region. Upon forward bias, free-carriers are selectively injected into the microdisk rim and spatially overlap with the WGM field, resulting in resonance tuning.

Figure 1 (b) shows the cross-sectional schematic of our lateral p-i-n diodes embedded microdisk (along the dashed line in Fig. 1 (a)). The microdisk radius is 10 μm and the n^+-doped region radius is 7 μm. The p^+-doped region has a 1-μm separation from the microdisk sidewall and a width of 4 μm.

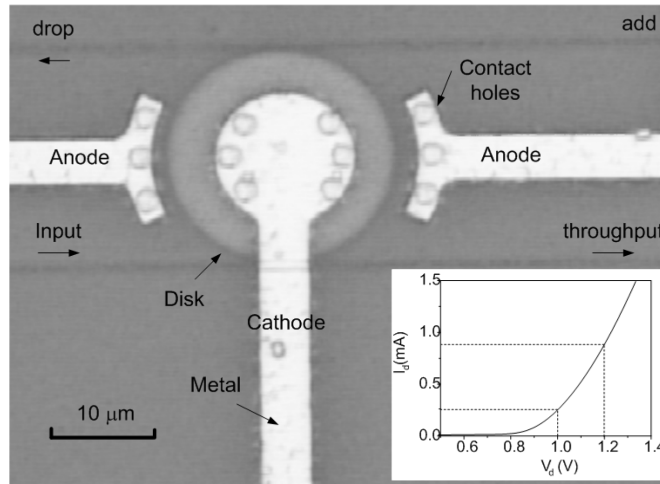

Fig.2. (a) Optical micrograph of a fabricated p-i-n integrated microdisk channel add-drop filter. The waveguide width is 0.3 μm and the air-gap separation in the coupling region is 0.35 μm. Inset shows the measured IV curve indicating a turn-on voltage of ~0.73 V.

Figure 2(a) shows the optical micrograph of the fabricated device. We used 0.2μm SOI wafer with 3-μm BOX layer for the device fabrication. We employed photolithography and RIE dry etching. The device height is ~0.15 μm with a slab height of ~0.05-μm. We implanted $3x10^{15}$ cm^{-2} phosphorous and boron dopants for the n^+ region and p^+ regions respectively. An upper cladding of 0.6-μm-thick low temperature oxide (LTO) was deposited as an electrical isolation layer. Aluminum is used for metal contact and the two p^+ arc regions are electrically connected. The inset shows the measured I-V curve. At 1V forward bias, the current flowing through the buried diodes is ~0.25 mA, which induces ~$6x10^{17}$ cm^{-3} extra carrier concentration (both electron and hole) in the intrinsic regions. At 1.2V forward bias, the current increases to 0.88 mA, resulting in ~$1.7x10^{18}$ cm^{-3} extra carrier concentrations. Our simulations based on MEDICI semiconductor simulator also suggest a uniform carrier distribution within the intrinsic region at 1V or 1.2V forward bias. Using the empirical free-carrier dispersion relation by Soref and Bennet [3], we calculate a refractive index change $\Delta n \approx -0.002$ and an absorption coefficient change $\Delta\alpha \approx 8.7$ cm^{-1} in the intrinsic region at drive voltage V_d = 1V. At V_d = 1.2V, the refractive index and absorption coefficient changes increase to $\Delta n \approx -0.004$ and $\Delta\alpha \approx 21.75$ cm^{-1}.

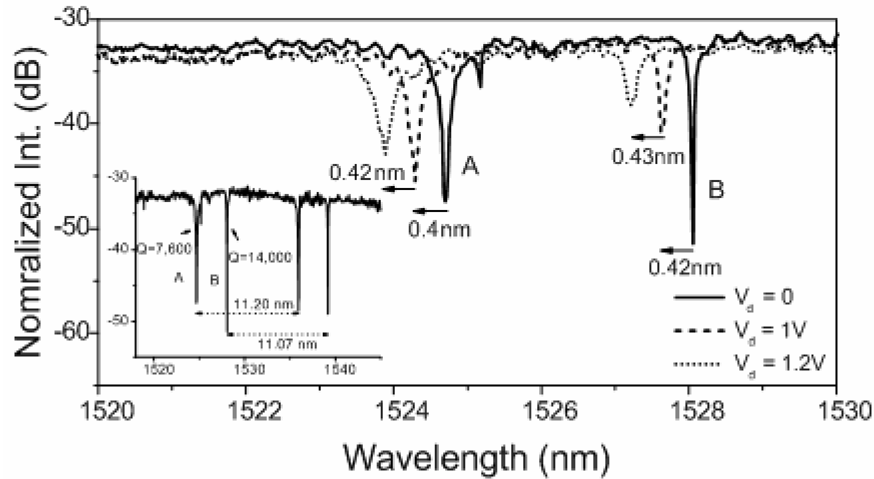

Fig.3. Electro-optical tuning of the throughput port modes A and B at three different DC voltages: V_d = 0 V (solid line), 1 V (dashed line) and 1.2 V (dotted line). Inset shows the expanded-range throughput port spectrum indicating different FSRs for modes A and B (V_d = 0 V).

Figure 3(b) shows the initially measured throughput-port spectra of TE polarization (**E** || device plane) with V_d = 0 V, 1 V, and 1.2 V. Inset shows an expanded-range spectrum at V_d = 0 V indicating a free spectral range (FSR). At V_d = 0 V, both modes A and B have a high extinction ratio exceeding 15 dB, yet mode A has a relatively low Q of 7600 and a FSR ≈ 11.20 nm, while mode B has a relatively high Q of 14000 and a FSR ≈ 11.07 nm. Higher order WGMs have a deeper field penetration toward disk center, and thus have a relatively short round trip length, which results in larger FSRs. Here, based on the FSRs of modes A and B, we deduce that mode A is a higher order mode compared with mode B. At V_d = 1 V, mode A has a blueshift of 0.4 nm, a slight linewidth broadening, and a ~1 dB reduction in the extinction ratio. In contrast, mode B has a blueshift of 0.42 nm, a similar degree of linewidth broadening, yet a ~10 dB reduction in the extinction ratio. At V_d = 1.2 V, both modes A and B display further blueshifts, linewidth broadening and a slight reduction in the extinction ratios. The resonance blueshift is consistent with the calculated $\Delta\lambda \approx 0.38$ nm. The linewidth broadening and extinction ratio reduction are expected from the $\Delta\alpha$, however further work is needed to address the significant mode dependence in the extinction ratio reduction.

In conclusion, we demonstrated an injection-type active SOI microdisk resonator device using selectively integrated p-i-n diodes. We successfully fabricated on a SOI substrate the waveguides laterally coupled 20-μm-diameter microdisk resonator. Our initial measurements show that upon 1 V forward bias of the embedded p-i-n diodes, 0.4 nm blueshift can be obtained, along with linewidth broadening, and mode dependent extinction ratio reduction. High-speed modulation response measurement is in progress.

References

[1] G T Reed and A P Knights, *Silicon Photonics: An Introduction* (John Wiley and Sons, 2004).

[2] Q. Xu, B. Schmidt, S. Pradhan and M. Lipson, "Micrometre-scale silicon electro-optic modulator," *Nature*, **435**, 325-327 (2005).

[3] R. A. Soref and B. R. Bennett, "Electrooptical effects in silicon", *IEEE J. Quant. Electron* **23**, 123-129 (1987).